

Position filtering-based non-orthogonal multiple access in mobile scenarios

Hao Qiu, Shaoshuai Gao

Abstract

In this paper, a downlink non-orthogonal multiple access (NOMA) system with partial channel state information (CSI) in mobile scenarios is considered. In particular, users are deployed randomly and move casually around the base station (BS). As a result, the channel gain of each user will vary as its position change, which has an influence on spectrum efficiency of conventional NOMA. For the addressed scenario, an analytical framework in terms of average sum rate performance is developed to evaluate the impact of estimated position deviation. To further improve the system performance, a novel NOMA scheme based on position filtering in mobile scenarios is proposed. Monte Carlo simulation is also provided to demonstrate the spectrum efficiency improvement compared with conventional NOMA and OMA schemes. And the results verify the accuracy of proposed analytical framework.

I. INTRODUCTION

Non-orthogonal multiple access (NOMA) has recently received considerable attention and has been recognized as a promising candidate for future wireless networks [1], [2]. It is considered not only to improve the spectral efficiency but also to support massive connectivity. Compared to conventional orthogonal multiple access (OMA), the key idea of NOMA is to realize multiple access (MA) by encouraging non-orthogonal resource allocation among multiple users. More users than the number of available orthogonal resource blocks, like time-, frequency- and code-resources, are supported. This can be achieved at the cost of increased receivers' complexity, which is needed to separate the signal of each user. The power-domain NOMA is inspired by the superposition coding technology, in which the signals of different users are multiplexed by using different power allocation (PA) coefficients. It should be noted that fairness is also a key property in NOMA that needs to be taken into consideration. In particular, the users with poor channel conditions are usually allocated more transmission power so that their signal can be

H. Qiu and S. Gao are with the School of Electronic, Electrical and Communication Engineering, the University of Chinese Academy of Sciences, Beijing 101408, China (email: qiuhaohao16@mails.ucas.ac.cn, ssgao@ucas.ac.cn).

decoded successfully by regarding the signals of others as noise. The successive interference cancellation (SIC) strategy is implemented at the users with better channel conditions. In other words, they decode the signals of poorer users first, remove them from the received superimposed signal, and then decode their own messages. On the other hand, NOMA can be easily combined with current communication technologies owing to the excellent compatibility with conventional OMA. For instance, downlink NOMA has been proposed in the 3rd generation partnership project long-term evolution (3GPP-LTE) system, where NOMA is referred to as multi-user superposition transmission (MUST) [3]. Furthermore, NOMA has been applied to the fourth digital TV standard (ATSC 3.0), where NOMA is referred to as layered division multiplexing (LDM) [4], [5].

A. Related Work and Motivation

The philosophy that NOMA can use spectrum more efficiently is motivated by the fact that the difference of channel conditions can be exploited by opportunistically allocating the transmission power [6]–[9]. In [6], the impact of path loss on the performance of NOMA with randomly deployed users was estimated, which has demonstrated that NOMA can outperform conventional OMA. The impact of user pairing on NOMA has been investigated in [7]. And it has been considered in two kinds of NOMA systems, i.e., NOMA with fixed power allocation (F-NOMA) and cognitive-radio-inspired NOMA (CR-NOMA). In [8], NOMA was investigated under different power allocation strategies from a fairness standpoint. The design of uplink NOMA has been proposed in [9] and the results have showed significant performance improvement to Orthogonal Frequency Division Multiple Access (OFDMA).

The concept of NOMA can also be linked to many communication technologies [10]–[14]. Specifically, NOMA is applied to a coordinated system in order to support the cell-edge users in [10]. The application of multiple-input multiple-output (MIMO) techniques to NOMA has been considered in [11], which has demonstrated that NOMA can be used to improve the spectrum efficiency of MIMO. According to the principle of SIC, the users with better channel conditions have to know the messages of other users first in order to decode their own messages. Such prior information can be exploited to improve the performance of poor users. As shown in [12], a cooperative NOMA scheme has been characterized by analyzing outage probability and diversity order. In [13], NOMA is employed in a large-scale underlay cognitive radio (CR) network. And a high-ratio visible light communication (VLC) system along with NOMA was also considered in [14].

Recently, a power allocation optimality problem in a downlink single-input single-output (SISO) NOMA system is investigated in [15]. To maximize the sum rate subject to the Quality of Service (QoS) requirement of each user, the optimal decoding order is determined by the channel conditions. In particular, it is preferable to decode the messages of the poor users first. Actually, most of the existing works in the open literatures about NOMA are under the assumption that both the BS and the users can obtain perfect knowledge of channel gains. In conventional communication systems, the CSI between BS and each user can be estimated by pilot signals. After estimating the channel from pilot signals, the users send the results back to the BS. However, in a fast time varying situation, this assumption might not be realistic since the amplitudes and the phases of the channel coefficients vary rapidly. This may also consume a substance amount of communication overhead, especially when there are too many users in the system. The distances between transceivers play a dominant role in the second order statistics (SOS) of wireless channels [16]. Compared to fading, distance information changes much more slowly and is easier to obtain. Therefore it is more realistic for the BS to have access to it without much complexity. Thus like previous works [16]–[18], we focus on NOMA with partial channel information.

In this paper, we consider a downlink single-cell NOMA network with partial CSI. Different from [16]–[18] where the position and path loss of each user is fixed, we concentrate on mobile scenarios. Users are deployed randomly around the BS and move casually. As a result, the path loss of each user is changing constantly and can be predicted to some extent. The impact of the position uncertainty on the performance of NOMA is investigated and a novel position filtering-based NOMA scheme is proposed. The main contributions of this paper is summarized in the next subsection.

B. Contribution

The main contributions of this article are summarized as follows:

- According to the sum rate approximation, we emphasize the importance of the decoding order in the NOMA under different channel conditions. Based on these results, the impact of position information deviation on the decoding order and average sum rate performance has been analyzed. We adopt a new metric, named as decoding order error probability (the probability that the user order is not optimal) to evaluate the affect of positioning deviation. For the most practical case of two-node pairing case, the analytical framework of the error

probability and average sum rate performance is proposed in both the fading-free scenario and the fading scenario. The results can act as a guide to a novel NOMA scheme and allow us to investigate the impact of system parameters.

- Since both the power allocation and decoding order are determined by distance information, more accurate position information is required. In this context, we propose a novel NOMA scheme based on position filtering in mobile scenarios to further improve the spectrum efficiency. The scheme includes two algorithms. In detail, the BS applies a self-adaptive filter, i.e. Kalman Filter [19], to track the movement of each user after observing the location of each user with a positioning method, such as global positioning system (GPS) or received signal strength (RSS) approaches [20]. Then according to the estimate results, a power allocation strategy is implemented at the BS and SIC decoding is carried out at the side of receivers. This algorithm is named as position-tracking based NOMA. In addition, position observation is not necessary at all slots in order to reduce network overhead. Instead, the previous position information and prior user mobile models can be used to predict user's movement in advance. Thus we present another algorithm called position-prediction based NOMA. This algorithm has led to a trade off between system performance and communication overhead. Comparing with position-tracking based NOMA, less channel information feedback is required while a suboptimal performance can also be guaranteed.
- Finally, we present Monte Carlo simulations to demonstrate the accuracy of analytical results and performance evaluation. From the simulation results, one can observe that our algorithms can improve the accuracy of distance information and a better sum rate performance can be obtained. By comparing to OMA and conventional NOMA, the novel NOMA scheme shows superior performance to the benchmarks. Additionally, position-prediction based NOMA can still achieve a great performance gain with relatively low network overhead.

C. Organization and Notations

The remainder of this paper is organized as follows. The system model is described and the factors that affect the spectrum efficiency of NOMA under different channel conditions are introduced in Section II. In Section III, the impact of estimated position deviation on NOMA average sum rate performance is evaluated. In Section IV, a novel position filtering based NOMA scheme is proposed. And computer simulation results and some discussions are presented in Section V. Finally, Section VI concludes the paper.

Throughout this paper, matrices and vectors are denoted by upper- and lower-case boldface letters respectively. The superscripts T denote transpose. Expectation is expressed by $E\{\cdot\}$ and probability is denoted by $\Pr(\cdot)$. In addition, $\mathcal{N}(\mathbf{a}, \mathbf{R})$ and $\mathcal{CN}(\mathbf{a}, \mathbf{R})$ denotes the distribution of real Gaussian random vectors and circularly symmetric complex Gaussian (CSCG) random vectors with mean vector \mathbf{a} , covariance matrix \mathbf{R} , respectively. \mathbf{I}_n denotes the identity matrix of size n . $\binom{n}{k}$ denotes a combination formula, i.e. $\frac{n!}{(n-k)!k!}$.

II. SYSTEM MODEL

In this paper, we focus on a single-cell downlink NOMA system in a mobile scenario, as shown in Fig.1. The network consists of one BS and M users U_i ($i = 1, 2, \dots, M$) where the BS and all the users are equipped with a single antenna. It is assumed that the BS is located at the origin of a two-dimensional Euclidean plane, expressed as \mathbb{R}^2 . At the beginning, users are deployed randomly and the distance between the BS and U_i is denoted by d_i ($i = 1, 2, \dots, M$). Similar to [17], [21], the original locations of users are modeled as homogeneous Poisson point process (HPPP) with density λ_a . In particular, they are uniformly distributed in the disk D with radius R_D . The number of users M follows a Poisson distribution with $\Pr(M = k) = (\mu^k/k!) e^{-\mu}$, where $\mu = \pi R_D^2 \lambda_a$ is the average number of users. After that, they are assumed to walk casually around the BS. It is worthy to point out that the zone that users can reach is not restricted to the disc D , shown in Fig.1(b). More details about mobility models will be described in Section IV. We assume that the BS always have messages to transmit to each user and the total transmission power is equal to P . For the channel model, all wireless channels in the network are assumed to be independent identically distributed (i.i.d) and quasi-static fading, i.e. the channel gain remains constant for a given coherence time and varies independently from one to another. The fading-free scenario and the fading scenario are both considered in this article. We use path loss to model the channel for the former. And a composite channel model is assumed in the fading scenario, which consists of large-scale path loss and small-scale fading. Thus the channel coefficient between user U_i and the base station can be denoted by $r_i = h_i/d_i^{\alpha/2}$, where $h_i \sim \mathcal{CN}(0, 1)$ and α is the path loss exponent. Therefore, the channel gain can be calculated as $|r_i|^2 = |h_i|^2 d^{-\alpha}$, in which $|h_i|^2$ is subjected to an exponential distribution with parameter 1.

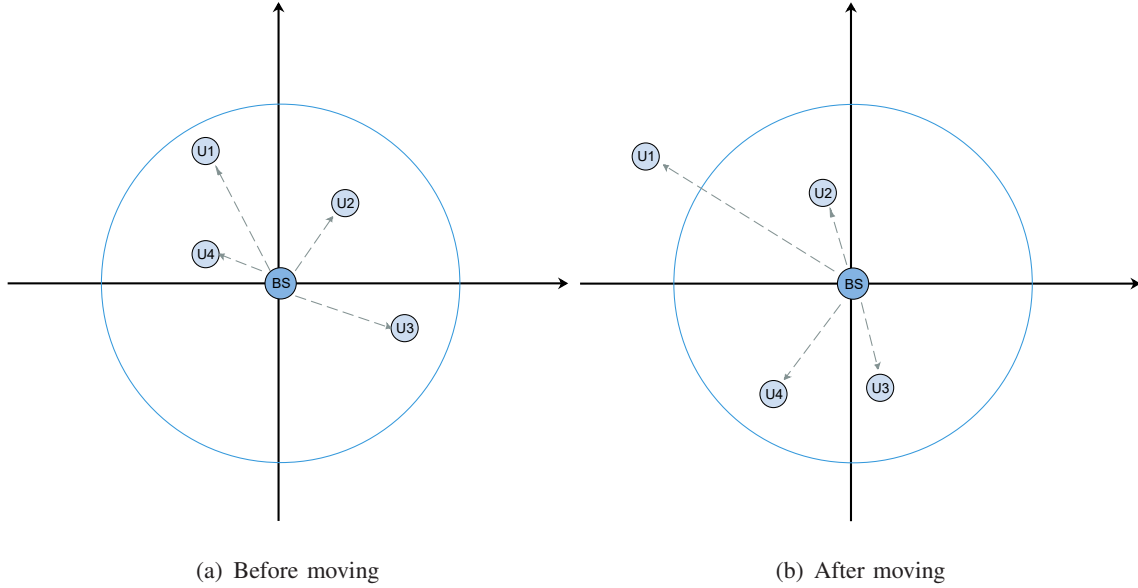


Fig. 1. An illustration of the assumed network model

A. NOMA Scheme with Partial Channel Information

In NOMA, the BS transmits messages to all users simultaneously. Hence without loss of generality, the distances can be sorted as follows

$$d_1 < d_2 < \dots < d_M \quad (1)$$

According to the principle of superposition coding, the signals of different users are superposed with distinct power. As a result, the signal S sent by the BS can be expressed as follows:

$$S = \sum_{m=1}^M \sqrt{\alpha_m P} S_m \quad (2)$$

where S_m ($m = 1, 2, \dots, M$) denotes the signal of the user U_m , α_m is power allocation factor that is subject to $\sum_{m=1}^M \alpha_m = 1$. At the side of receivers, the signal received by user U_m can be formulated as

$$y_m = r_m \sum_{l=1}^M \sqrt{\alpha_l P} S_l + n_m \quad (3)$$

where n_m denotes the Gaussian noise of user m . And the noise is assumed to be normalized with zero mean and variance σ_n^2 , i.e. $n_m \sim \mathcal{CN}(0, \sigma_n^2)$. Based on (3), if SIC is carried out by user m , U_m has to detect the messages of U_l ($m+1 \leq l \leq M$) successfully before detecting his own message. In other words, U_m have to decode the message of U_M first. And if the message of U_M is decoded successfully, the signal will be removed from the received composite signal,

step by step until U_m can detect his own message. Under the assumption of perfect channel estimation at receivers, the achievable rate for U_m to detect the signal S_l is shown as follows

$$R_{m \rightarrow l} = \log_2 \left(1 + \frac{|r_m|^2 \alpha_l}{|r_m|^2 a_{l-1} + \frac{1}{\rho}} \right) \quad (4)$$

where $a_{l-1} = \sum_{k=1}^{l-1} \alpha_k$, $a_0 = 0$, and $\rho = \frac{P}{\sigma_n^2}$ denotes the transmit SNR.

Suppose that the user U_m is capable of detecting the message of each U_l ($m+1 \leq l \leq M$) correctly and perfect SIC is assumed. Thus the achievable rate of U_m is given by

$$R_m = \log_2 \left(1 + \frac{|r_m|^2 \alpha_m}{|r_m|^2 a_{m-1} + \frac{1}{\rho}} \right) \quad (5)$$

Especially, interference does not exist when U_1 detect the signal S_1 . So the achievable rate is expressed as

$$R_1 = \log_2 (1 + \rho |r_1|^2 \alpha_1) \quad (6)$$

It should be noted that as for two different users U_i and U_j , if $|h_i|^2 \geq |h_j|^2$, we have the following property for achievable rate.

$$\begin{aligned} R_{i \rightarrow j} &= \log_2 \left(1 + \frac{|r_i|^2 \alpha_j}{|r_i|^2 a_{j-1} + \frac{1}{\rho}} \right) \\ &> \log_2 \left(1 + \frac{|r_j|^2 \alpha_j}{|r_j|^2 a_{j-1} + \frac{1}{\rho}} \right) = R_j \end{aligned} \quad (7)$$

Similarly, if $|h_i|^2 \leq |h_j|^2$, vice versa. In other words, the achievable rate of a signal is restricted by the user with the poorest channel condition who needs to detect it¹. Furthermore, average sum rate is used as a performance criteria for the case when the transmitted data rates are determined according to real-time channel conditions. In terms of NOMA with partial channel information, assuming that user U_m always decodes the signals S_l ($m+1 \leq l \leq M$) correctly, the sum rate of the system can be expressed as follows

$$\begin{aligned} R_{sum}^I &= \sum_{l=1}^M \min_{1 \leq m \leq l} R_{m \rightarrow l} \\ &= \sum_{l=1}^M \min_{1 \leq m \leq l} \left(1 + \frac{|r_m|^2 \alpha_l}{|r_m|^2 a_{l-1} + \frac{1}{\rho}} \right) \end{aligned} \quad (8)$$

¹As a special case, the achievable rate of a user's signal is restricted by himself only if users are ordered by perfect CSI, such as [6], [7]. However under the assumption of partial CSI, the property $|r_i|^2 < |r_j|^2$ cannot be guaranteed despite of $d_i < d_j$. And the property is also considered in [15].

As a comparison, the sum rate performance of OMA scheme can be calculated as

$$R_{sum}^{II} = \sum_{l=1}^M \frac{1}{M} \log_2 (1 + \rho |r_m|^2) \quad (9)$$

This can be used as a benchmark in order to compare with the NOMA system in section V.

B. Factors Affecting NOMA Spectrum Efficiency under Different Channel Conditions

In this subsection, the spectrum efficiency of NOMA under different channel conditions is considered. For a brief explanation, we assume the BS transmits messages to two users simultaneously. The two users are denoted by U_1 and U_2 respectively and the decoding order is from U_2 to U_1 . That means U_1 firstly detects the signal S_2 while referring to S_1 as interference according to the SIC strategy. Meanwhile U_2 detect the signal S_2 directly regarding S_1 as noise. In this case, the sum rate can be expressed as follows

$$R_{sum}^I = \log_2 (1 + \rho |r_1|^2 \alpha_1) \quad (10)$$

$$+ \log_2 \left(1 + \frac{\min (|r_1|^2, |r_2|^2) \alpha_2}{\min (|r_1|^2, |r_2|^2) \alpha_1 + \frac{1}{\rho}} \right)$$

Under the condition of high SNR, i.e. $\rho \rightarrow \infty$, sum rate can be approximated as

$$R_{sum}^I \approx \log_2 (1 + \rho |r_1|^2 \alpha_1) + \log_2 \left(1 + \frac{\alpha_2}{\alpha_1} \right)$$

$$= \log_2 (\rho |r_1|^2) \quad (11)$$

The result implies that when SNR is high, the dominant factor of NOMA sum rate performance is the channel conditions whose signals are detected later. This is because the user U_2 is interference-limited if the SNR is high enough, whose achievable rate is mainly restricted by power allocation strategy as shown in (11). On the contrary the user U_1 is noise-limited, whose channel conditions have a more significant affect on system performance.

On the other hand, under the condition of low SNR, i.e. $\rho \rightarrow 0$, we have

$$R_{sum}^I \approx \log_2 (1 + \rho |r_1|^2 \alpha_1)$$

$$+ \log_2 (1 + \rho \min (|r_1|^2, |r_2|^2) \alpha_2) \quad (12)$$

Based on (12), user U_1 and U_2 are both noise-limited when SNR is low, which implies that the sum rate performance of NOMA is influenced by both the channel conditions and power allocation scheme. Furthermore, larger spectrum efficiency can be achieved if the signal of the

strong user is decoded later. And the optimal sum rate performance can be achieved by traditional water-filling algorithm according to (12).

The results above can also be extended to the case of multiple users similarly. As we can see, the detection order plays an important part in NOMA spectrum efficiency at both high SNR region and low SNR region. And how to arrange the detection order and improve system spectrum efficiency with acceptable complexity is an interesting issue, which is considered in the next section.

III. POSITION ESTIMATION AND PERFORMANCE ANALYSIS

Suppose that there are M users around the base station and they are ordered according to their distances to the BS as shown in (1). And the distance information of user U_i obtained by the BS can be denoted by \hat{d}_i . For mathematical tractability, we consider the case where the BS schedules two users to transmit messages like [7]. The two users are selected to be paired for implementation of the NOMA. Without loss of generality, it is assumed that user U_1 and U_2 are paired and $d_1 < d_2$. Besides, suppose that the estimated position deviations of axis-x and axis-y in a Cartesian coordinate are subject to a Gaussian distribution with zero mean and variance σ^2 . The results of position estimation will lead to a distinct decoding process and system performance, which can be seen from analysis and simulation results below.

In this article, we adopt a new metric to evaluate the impact of distance deviation, which is named as decoding order error probability. It is defined as the probability that the decoding order isn't optimal², which is due to incomplete channel information and estimate deviation.

Lemma 1. *In the fading-free scenario, the decoding order error probability of NOMA with partial channel information for the two pairing users with fixed locations can be expressed as follows*

$$P_e^1 = \sum_{i=0}^{\infty} \sum_{j=0}^{\infty} P_{\lambda_1\beta}(i) P_{\lambda_2\beta}(j) I_{i,j} \quad (13)$$

where $P_{\lambda}(k) = \frac{e^{-\lambda}\lambda^k}{k!}$ ($k \geq 0$) is the probability mass function (PMF) of a Poisson distribution, $\lambda_k = d_k^2$ ($k = 1, 2$), $\beta = \frac{1}{2\sigma^2}$, and $I_{i,j} = \left(\frac{1}{2}\right)^{\alpha_i+\alpha_j} \binom{\alpha_i+\alpha_j-1}{\alpha_j} F\left(1, \alpha_i + \alpha_j, \alpha_j + 1, \frac{1}{2}\right)$, $\alpha_k = k + 1$, $F(\cdot)$ denotes a hypergeometric function.

²The optimal decoding order has been investigated in [15]

Proof. Assume that the real position of a user is represented as (x, y) and the estimated position is given by (\hat{x}, \hat{y}) . Thus the real distance is $d^2 = x^2 + y^2$ and the measured distance is $\hat{d}^2 = \hat{x}^2 + \hat{y}^2$. Recall that the estimated position deviation is subjected to a Gaussian distribution, i.e. $\hat{x} \sim \mathcal{N}(x, \sigma^2)$ and $\hat{y} \sim \mathcal{N}(y, \sigma^2)$. Therefore, \hat{d} is subjected to a non-central chi-squared distribution. The PDF is given as follows

$$f_{\hat{d}}(x) = \frac{1}{2\sigma^2} \exp\left(-\frac{x+\lambda}{2\sigma^2}\right) I_0\left(\frac{\sqrt{x\lambda}}{\sigma^2}\right), (x \geq 0) \quad (14)$$

where $\lambda = d^2 = x^2 + y^2$, $I_0(x)$ denotes zero-order modified Bessel function of the first kind. Express it in the form of a series and substitute into (14), we have

$$\begin{aligned} f_{\hat{d}}(x) &= \frac{1}{2\sigma^2} \exp\left(-\frac{x+\lambda}{2\sigma^2}\right) \sum_{k=0}^{\infty} \frac{1}{k! \Gamma(k+1)} \left(\frac{\sqrt{x\lambda}}{2\sigma^2}\right)^{2k} \\ &= \sum_{k=0}^{\infty} P_{\lambda\beta}(k) f_{\alpha_k, \beta}(x) \end{aligned} \quad (15)$$

where $\alpha_k = k + 1$, $\beta = \frac{1}{2\sigma^2}$, $P_{\lambda}(k) = \frac{e^{-\lambda} \lambda^k}{k!}$ ($k \geq 0$) is the probability mass function (PMF) of a Poisson distribution, $f_{\alpha, \beta}(x) = \frac{\beta^\alpha x^{\alpha-1} e^{-\beta x}}{\Gamma(\alpha)}$, ($x > 0$) is the PDF of Gamma distribution with parameters α and β . (15) indicates that the PDF of \hat{d} is a weighted sum of the Gamma distribution PDF, whose weight coefficients are the probabilities of Poisson distributions. Thus its CDF can be calculated naturally as

$$F_{\hat{d}}(x) = \sum_{k=0}^{\infty} P_{\lambda\beta}(k) F_{\alpha, \beta}(x) \quad (16)$$

where $F_{\alpha, \beta}(x) = \frac{\gamma(\alpha, \beta x)}{\Gamma(\alpha)}$ is the CDF of Gamma distribution and is expressed as the form of a regularized Gamma function. Recall that the two positions are fixed and $d_1 < d_2$, thus we have $\lambda_1 < \lambda_2$. In this case, the decoding order error event occurs only if the order of the estimated distances is incorrect, i.e. $\{\hat{d}_1 < \hat{d}_2\}$. Let $P_e = \Pr(\hat{d}_1 < \hat{d}_2)$. The error probability can be formulated as

$$P_e^1 = P_e = \int_0^{+\infty} \int_0^u f_{\hat{d}_1}(u) f_{\hat{d}_2}(v) dv du \quad (17)$$

Substitute (15) to (17), a double integral will be obtained, the inner integral result is the CDF of Gamma distribution as shown in (16). After some simplification, we obtain the expression

shown in (13). And the integral term $I_{i,j}$ can be calculated as follows

$$\begin{aligned}
I_{i,j} &= \int_0^\infty f_{\alpha_i,\beta}(x) F_{\alpha_j,\beta}(x) dx \\
&= \int_0^\infty \frac{\beta^{\alpha_i} x^{\alpha_i-1} e^{-\beta x}}{\Gamma(\alpha_i)} \frac{\gamma(\alpha_j, \beta x)}{\Gamma(\alpha_j)} dx \\
&= \frac{\beta^{\alpha_i}}{\Gamma(\alpha_i) \Gamma(\alpha_j)} \int_0^\infty x^{\alpha_i-1} e^{-\beta x} \gamma(\alpha_j, \beta x) dx \\
&\stackrel{(a)}{=} \frac{\beta^{\alpha_i}}{\Gamma(\alpha_i) \Gamma(\alpha_j)} \frac{\beta^{\alpha_j} \gamma(\alpha_i + \alpha_j)}{\alpha_j (2\beta)^{\alpha_i + \alpha_j}} F\left(1, \alpha_i + \alpha_j, \alpha_j + 1, \frac{1}{2}\right) \\
&= \left(\frac{1}{2}\right)^{\alpha_i + \alpha_j} \binom{\alpha_i + \alpha_j - 1}{\alpha_j} F\left(1, \alpha_i + \alpha_j, \alpha_j + 1, \frac{1}{2}\right) \tag{18}
\end{aligned}$$

where the calculation process (a) in (18) is obtained by using the result (6.455) in [22]. And $F(\cdot)$ denotes a hypergeometric function. After substituting (15), (16) and (18) into (17), the proof is completed. \square

Remark 1: Lemma 1 indicates that the decoding order error probability can be expressed as a weighted summation of $I_{i,j}$, whose weight coefficients are the probabilities of Poisson distribution. Note that the term $I_{i,j}$ is just a function of the series' indices in (13), i.e. i and j , which means it can be used to simplify the calculation. Furthermore, it can be approximated as a finite sum of finite terms due to the convergence property. And the results of (13) can also be used to calculate the average sum rate performance of NOMA for analytical tractability.

Remark 2: As shown in Lemma 1, the decoding order error probability is effected by the distances of users and positioning deviation. Intuitively, as the difference between the two distances gets smaller or positioning deviation gets larger, the error probability P_e will become larger and deteriorate the performance of NOMA, which will be illustrated below.

Lemma 2. *In the fading-free scenario, the sum rate performance of NOMA with partial channel information for the two pairing users with fixed locations can be formulated as follows*

$$\begin{aligned}
R_{sum}^I &= \log_2 \left(1 + \frac{|r_2|^2 \alpha_2}{|r_2|^2 \alpha_1 + \frac{1}{\rho}} \right) \\
&\quad + (1 - P_e) \log_2 (1 + \rho |r_1|^2 \alpha_1) \\
&\quad + P_e \log_2 (1 + \rho |r_2|^2 \alpha_1) \tag{19}
\end{aligned}$$

where the probability P_e has been calculated in Lemma 1.

Proof. Please refer to Appendix A. \square

Remark 3: From lemma 2, one can observe that the first term of the sum rate formula is constant while the sum of the last two terms is a weighted summation. Note that the channel of user U_1 is better than that of U_2 in the fading-free scenario. As a result, the decoding order error will lead to the degradation of NOMA sum rate performance. From another perspective, this also indicates that the upper bound performance can be achieved if the users are ranked by perfect channel information, which is impracticable actually.

As for the fading scenario, the results are similar. Although we can not always ensure that the composite channel gains are dominated by distance, the near users are more likely to have better channel conditions. More specifically, the analytical framework of the fading scenario is shown in Lemma 3.

Lemma 3. *As for NOMA with partial CSI for the two pairing users with fixed locations in the fading scenario, the decoding order error probability is expressed as*

$$P_e^2 = \frac{D-1}{D+1}P_e + \frac{1}{D+1} \quad (20)$$

And the average sum rate performance can be calculated as follows

$$\begin{aligned} R_{sum}^I &= \varphi(2, \rho) + \varphi(1, \rho) \\ &+ (1 - P_e) [\varphi'(1, \rho\alpha_1) - \varphi(1, \rho\alpha_1) - \varphi(2, \rho\alpha_1)] \\ &+ P_e [\varphi'(2, \rho\alpha_2) - \varphi(1, \rho\alpha_2) - \varphi(2, \rho\alpha_2)] \end{aligned} \quad (21)$$

Where $D = d_2^2/d_1^2$, $\varphi(n, \phi) = -\frac{\lambda_n}{\lambda \ln 2} e^{\frac{\lambda}{\phi}} \text{Ei}\left(-\frac{\lambda}{\phi}\right)$ and $\varphi'(n, \phi) = -\frac{1}{\ln 2} e^{\frac{\lambda}{\phi}} \text{Ei}\left(-\frac{\lambda}{\phi}\right)$, $\lambda_k = d_k^2$ ($k = 1, 2$), $\lambda = \lambda_1 + \lambda_2$, $\text{Ei}(x)$ denotes an exponential integral. The probability P_e has been calculated in Lemma 1.

Proof. Please refer to Appendix B. □

Remark 4: The error probability and sum rate performance of NOMA in the fading scenario are given in Lemma 3. One can infer from (20) that the error probability is larger than that of the fading-free scenario. And the decoding order error event may still occur without any positioning deviation, i.e. $P_e = 0$, due to the incomplete CSI. Besides, the sum rate expression in (21) has the same form as (19), which shows the affect of user order on the NOMA sum rate is similar to that in the fading-free scenario. And the analytical result comparison between the fading-free and fading scenarios will be shown in section V.

In this section, we have analyzed the impact of positioning deviation on the NOMA sum rate performance when only partial CSI is available. Inaccurate distance estimation may make the SIC strategy suboptimal. The results have shown that more reliable position information is vital to improve system performance. Based on this, we propose a novel NOMA scheme based on position filtering in the next section, where the actions of users are predictable and this knowledge can be exploited to improve the system performance.

IV. POSITION FILTERING BASED NOMA SCHEME

In this section, we propose a novel scheme of position filtering based NOMA in mobile scenarios. Consider the single-cell network described in Section II, users can move casually around the base station. And the BS can gain the partial CSI with some positioning methods like GPS, then transmit different messages to all users simultaneously with these knowledge.

A. User Mobile Model

In this paper, the motion of users are described by a velocity sensor model [20]³. This mobile model can be expressed by a continuous-time state-space model. Suppose that the mobile state of a user is defined by a vector

$$\mathbf{s}(t) = [x(t), v_x(t), y(t), v_y(t)]^T \quad (22)$$

where $x(t)$ and $y(k)$ specify the position at time t in Cartesian coordinate. And $v_x(t)$ and $v_y(t)$ denote the velocity in x-axis and y-axis respectively. Thus the distance between the user and the base station can be calculated as

$$d(t) = x^2(t) + y^2(t) \quad (23)$$

In addition, the velocities can change at any time. The variation can be expressed by a white noise stochastic process vector $\mathbf{w}(t)$ and its covariance matrix is denoted by \mathbf{Q} .

$$\mathbf{w}(t) = [w_x(t), w_y(t)]^T \quad \mathbf{Q} = \sigma_w^2 \mathbf{I}_2 \quad (24)$$

And the state transition model is expressed with a linear differential equation as follows

$$\dot{\mathbf{s}}(t) = \tilde{\mathbf{A}}\mathbf{s}(t) + \tilde{\mathbf{B}}\mathbf{w}(t) \quad (25)$$

³Other more complicated models can also be involved such as dynamic mobile state model [23], though their results may be similar. And the design for practical outdoor scenarios is a promising future direction, but it is beyond the scope of this paper.

Where $\tilde{\mathbf{A}}$ and $\tilde{\mathbf{B}}$ are state-transition matrix and random input matrix respectively, are presented as

$$\tilde{\mathbf{A}} = \begin{bmatrix} 0 & 1 & 0 & 0 \\ 0 & 0 & 0 & 0 \\ 0 & 0 & 0 & 1 \\ 0 & 0 & 0 & 0 \end{bmatrix} \quad \tilde{\mathbf{B}} = \begin{bmatrix} 1 & 0 \\ 0 & 0 \\ 0 & 1 \\ 0 & 0 \end{bmatrix} \quad (26)$$

At time t , a measurement of the state vector is made according to

$$\mathbf{z}(t) = \mathbf{H}\mathbf{s}(t) + \mathbf{n}(t) \quad (27)$$

Where \mathbf{H} is the observation matrix, and is presented as

$$\mathbf{H} = \begin{bmatrix} 1 & 0 & 0 & 0 \\ 0 & 0 & 1 & 0 \end{bmatrix} \quad (28)$$

$\mathbf{n}(t)$ is the observation noise which is assumed to be zero mean Gaussian white noise process with covariance matrix $\tilde{\mathbf{R}} = \sigma_{ob}^2 \mathbf{I}_2$

After sampling the state and measurement vector once every T seconds, the model can be transformed into discrete-time state-space model. Let $\mathbf{s}_k = \mathbf{s}(kT)$ and $\mathbf{z}_k = \mathbf{z}(kT)$, we have

$$\mathbf{s}_{k+1} = \mathbf{A}\mathbf{s}_k + \mathbf{w}_k \quad (29)$$

Where

$$\mathbf{A} = e^{\tilde{\mathbf{A}}T} = \begin{bmatrix} 1 & T & 0 & 0 \\ 0 & 1 & 0 & 0 \\ 0 & 0 & 1 & T \\ 0 & 0 & 0 & 1 \end{bmatrix} \quad (30)$$

$$\mathbf{w}_k = \int_{kT}^{(k+1)T} e^{\tilde{\mathbf{A}}((k+1)T-\tau)} \tilde{\mathbf{B}}\mathbf{w}(\tau) d\tau \quad (31)$$

Where \mathbf{w}_k is a zero mean discrete-time Gaussian white noise vector, thus $E\{\mathbf{w}_n \mathbf{w}_{n+i}^T\} = 0$ for $i \neq 0$. Besides, the covariance matrix \mathbf{R} is calculated as

$$\mathbf{R} = E\{\mathbf{w}_n \mathbf{w}_n^T\} = \begin{bmatrix} T\sigma_w^2 & 0 & 0 & 0 \\ 0 & 0 & 0 & 0 \\ 0 & 0 & T\sigma_w^2 & 0 \\ 0 & 0 & 0 & 0 \end{bmatrix} \quad (32)$$

Based on this, we propose a novel downlink NOMA scheme with partial CSI in mobile scenarios. Position estimation is carried out with the help of a Kalman filter, which is based on minimizing error covariance. Let $\hat{\mathbf{s}}_k$ denote the estimated state vector. The purpose of the scheme is to obtain the optimal estimated distance in the sense of linear quadratic estimation and improve the system spectrum efficiency. According to the principle of Kalman filter, we propose two kinds of NOMA algorithms, i.e position-tracking based NOMA and position-prediction based NOMA. In position-tracking based NOMA, position measurement is carried out every slot the BS transmits messages. However, there may be insufficient measurement samples in realistic systems. In order to solve this issue and further reduce communication overhead, the distance information can be predicted with previous measurements and user's motion model obtained by the BS. Thus in position-prediction based NOMA, positioning is not carried out at each slot. Instead, the user order and power allocation scheme are determined by position prediction most of the time. The two schemes are specified as follows.

B. Position-tracking based NOMA

In position-tracking based NOMA, position observation is required at each slot. The algorithm can be divided to two steps as follows

Step 1: According to the user's state vector, covariance matrix of the last slot and the measurement data of the current slot, Kalman filter algorithm is performed to obtain the optimal position estimate. Then calculate the distance information by substituting the result into (23).

Step 2: According to the position estimate results, it is assumed that $\hat{d}_1 \leq \hat{d}_2 \leq \dots \leq \hat{d}_M$ without loss of generality. At the side of the BS, power allocation is conducted based on a predefined strategy or the QoS requirement of users. While at the side of receivers, decoding is carried out starting from the signal of the farthest user to that of the nearest user. And messages of each user can be obtained by SIC strategy.

The detailed algorithm procedure is described in table I.

C. Position-prediction based NOMA

In this subsection, we consider a more realistic scenario. As we know, transmitting the CSI to the BS may result in a mount of communication overhead and extra transmission delay. Thus the position information may not be available at every slot due to these reasons. Based on these, we propose the position-prediction based NOMA scheme. In the process of position estimation,

TABLE I
ALGORITHM 1: POSITION-TRACKING BASED NOMA

Initialization

Set initial predicted state estimate $\hat{\mathbf{S}}_{1|0} = \mathbf{0}$ and predicted error covariance $\mathbf{P}_{1|0} = \mathbf{I}_4$

Step 1:

For each user U_i

Calculate the Kalman gain:

$$\mathbf{K}_k = \mathbf{P}_{k|k-1} \mathbf{H} (\mathbf{H} \mathbf{P}_{k|k-1} \mathbf{H}^T + \mathbf{R})^{-1}$$

Updated state equation:

$$\hat{\mathbf{S}}_{k|k} = \hat{\mathbf{S}}_{k|k-1} + \mathbf{K}_k (\mathbf{z}_k - \mathbf{H} \hat{\mathbf{S}}_{k|k-1})$$

Updated estimate covariance:

$$\mathbf{P}_{k|k} = (\mathbf{I}_4 - \mathbf{K}_k \mathbf{H}) \mathbf{P}_{k|k-1}$$

Calculate the estimate distance:

$$\hat{d}_k = \hat{x}_k^2 + \hat{y}_k^2$$

Predicted state equation:

$$\hat{\mathbf{S}}_{k+1|k} = \mathbf{A} \hat{\mathbf{S}}_{k|k}$$

Predicted error covariance:

$$\mathbf{P}_{k+1|k} = \mathbf{A} \mathbf{P}_{k|k} \mathbf{A}^T + \mathbf{Q}$$

End

Step 2:

At the side of the transmitter, the BS ranks the users according to the estimate distances $\hat{d}_1 \leq \hat{d}_2 \leq \dots \leq \hat{d}_M$. Then the transmission power is assigned to each user accordingly.

At the side of the receivers, for each user U_i

let $l = M$, detect the signal S_l that is transmitted to U_l

- 1) If the detection is successful, the interference signal can be removed by SIC. Then let $l = l - 1$ and step by step until the user detects his own message.
- 2) If the detection is unsuccessful, the user fails to detect the message he needs.

End

some knowledge about the motions can be obtained by the BS. And this kind of knowledge can be used to predict users' position in the future. Thus in this case, a practical NOMA scheme with lower communication overhead is proposed while a reliable system performance also can be guaranteed.

Similar to position-tracking based NOMA, this scheme can be described in two steps. In step 1, if the BS has access to the measurement result, the Kalman filter is also performed as described in algorithm I. On the contrary, the BS will predict the position position of each user in the

future according to the prior model and previous measurement results if no measurement data is available. In step 2, the NOMA algorithm is carried out in the same way as position-tracking based NOMA.

The detailed algorithm procedure is shown in table II.

TABLE II
ALGORITHM 2: POSITION-PREDICTION BASED NOMA

Initialization

Set initial predicted state estimate $\hat{\mathbf{S}}_{1|0} = \mathbf{0}$ and predicted error covariance $\mathbf{P}_{1|0} = \mathbf{I}_4$

Recursion steps

Step 1:

For each user U_i

If the BS has access to the measurement data

Calculate the Kalman gain:

$$\mathbf{K}_k = \mathbf{P}_{k|k-1} \mathbf{H} (\mathbf{H} \mathbf{P}_{k|k-1} \mathbf{H}^T + \mathbf{R})^{-1}$$

Updated state equation:

$$\hat{\mathbf{S}}_{k|k} = \hat{\mathbf{S}}_{k|k-1} + \mathbf{K}_k (\mathbf{z}_k - \mathbf{H} \hat{\mathbf{S}}_k)$$

Updated estimate covariance:

$$\mathbf{P}_{k|k} = (\mathbf{I}_4 - \mathbf{K}_k \mathbf{H}) \mathbf{P}_{k|k-1}$$

End

Calculate the estimate distance:

$$\hat{d}_k = \hat{x}_k^2 + \hat{y}_k^2$$

Predicted state equation:

$$\hat{\mathbf{S}}_{k+1|k} = \mathbf{A} \hat{\mathbf{S}}_{k|k} \text{ or } \hat{\mathbf{S}}_{k+1|k} = \mathbf{A} \hat{\mathbf{S}}_{k|k-1}$$

Predicted error covariance:

$$\mathbf{P}_{k+1|k} = \mathbf{A} \mathbf{P}_{k|k} \mathbf{A}^T + \mathbf{Q} \text{ or } \mathbf{P}_{k+1|k} = \mathbf{A} \mathbf{P}_{k|k-1} \mathbf{A}^T + \mathbf{Q}$$

End

Step 2 is the same as that in Algorithm 1

V. NUMERICAL RESULTS AND SIMULATIONS

In this section, numerical results and Monte Carlo simulations are provided to validate the correctness of our analytical results and evaluate the performance of the proposed novel NOMA scheme. The parameters used in our simulations are set as follows. The sampling interval is set to $T = 0.2s$ and each sample trajectory includes $K = 300$ sample points, which corresponds to the duration of each independent trial $1min$. The radius of the disk D where users are

deployed at the beginning is set as $R_D = 30m$. The variance of process noise is $\sigma_w^2 = 5$. As for channels, the path loss exponent is fixed to $\alpha = 2$. The small-scale fading is assumed to be Rayleigh fading which means $h_i \sim \mathcal{CN}(0, 1)$. And the power allocation factors in NOMA are $\alpha_k = \frac{2^{k-1}}{\sum_{l=1}^M (2^{l-1})}$, $1 \leq k \leq M$. The thermal noise is set as $\sigma_n^2 = -30dBm$. The Monte Carlo simulation results are averaged over 10^5 independent trials.

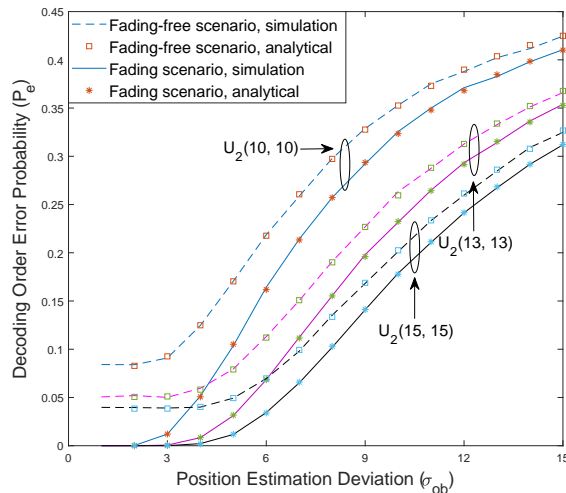


Fig. 2. The decoding order error probability versus estimated position deviation with two users and fixed user position $U_1(3, 3)$.

In Fig. 2, the impact of estimate deviation on the detection order error probability P_e is investigated. As observed from Fig. 2, the error probability P_e increases as deviation becomes larger. This is because the uncertainty of position estimate will cause incorrect user order. Furthermore, the user order is more likely to be disordered and the error probability is higher when users are getting closer. It is worth to point out that the curves reveal distinct properties under different channel models. As for the fading scenario, an error floor can still be observed even with very low estimate deviation. This is because the channel condition of a user is not just determined by the distance to the BS. Incomplete channel information can lead to an incorrect decision on user decoding order. Thus detection order error event may still occur when the estimate deviation doesn't exist. And the approximated analytical results in (13) match with Monte Carlo simulation.

Fig. 3 demonstrates the influence of estimated position deviation on NOMA average sum rate performance and compare it with OMA scheme. As observed from Fig. 3(a) and Fig. 3(b), one can see that the impact of position deviation is similar under the two kinds of channel model. In particular, the average sum rate performance deteriorates when the observation noise variance

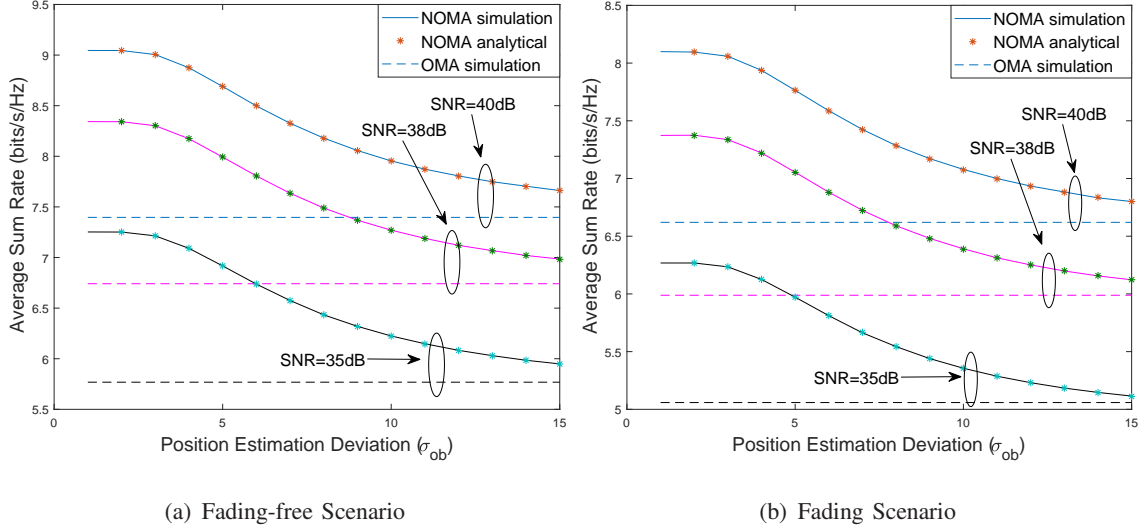


Fig. 3. Impact of position observation noise on average sum rate under different transmit SNR with $M = 2$ and fixed user position $U_1(3, 3), U_2(10, 10)$.

σ_{ob}^2 is increasing since the higher decoding order error probability P_e will reduce the sum rate. And the sum rate of the fading scenario is a bit lower than that of the fading-free scenario due to the effect of small-scale fading. Additionally, the comparison with OMA shows that the performance gain of NOMA can still be guaranteed in spite of the existence of estimation error. And the correctness of analytical result in (19) is also validated by the Monte Carlo simulation.

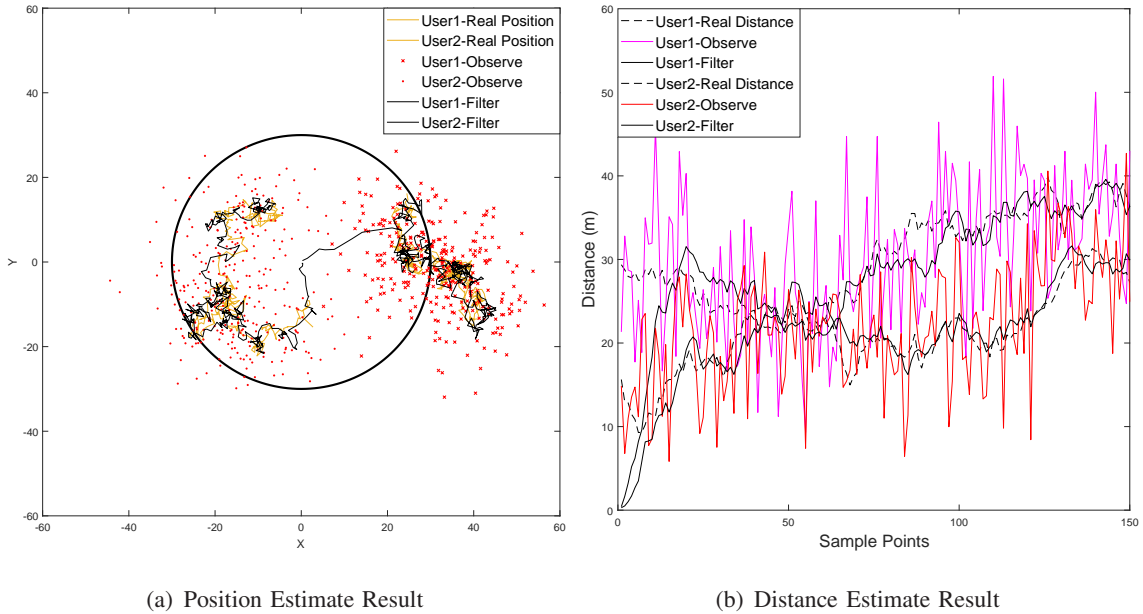


Fig. 4. A diagram of one simulation trial result where the number of users $M = 2$

Fig. 4 demonstrates the position estimate process in one simulation trial, in which there are two users in the network. As shown in Fig. 4(a), the estimate motion trajectory after filtering is close to the real one while the observation points with noise are around the real position points. From Fig. 4(b), the distances after filtering also approach the real values. And compared to the distances directly calculated by the observations positions, the relation between the two users' distances is more accurate. As a result, the error probability P_e will be much smaller and the performance is improved, which will be demonstrated below.

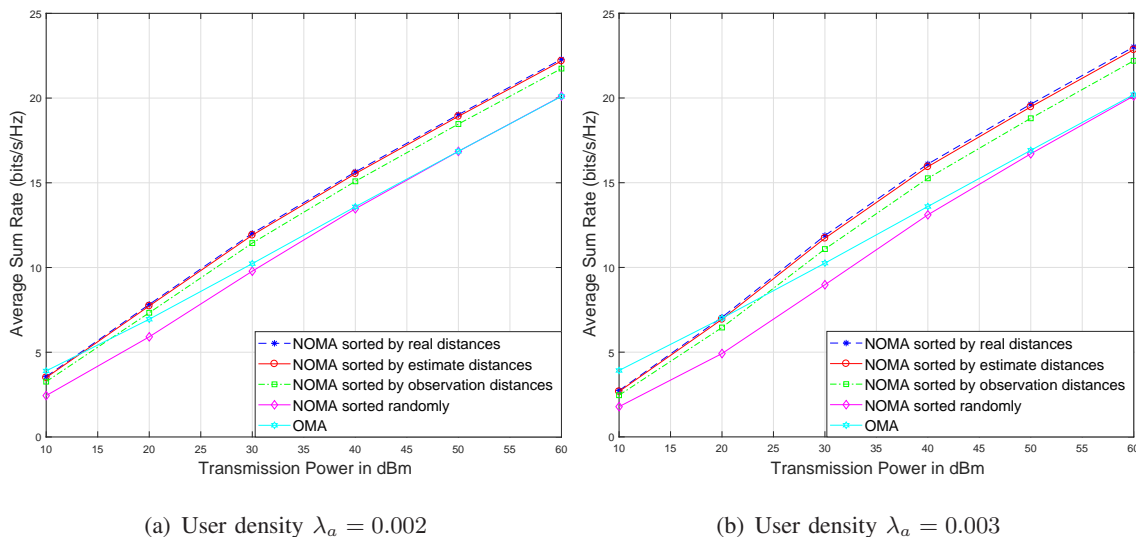


Fig. 5. Average sum rate performance of position-tracking based NOMA with observation noise variance $\sigma_{ob}^2 = 50$.

In Fig. 5, we show the simulation results for sum rate performance of position-tracking based NOMA in mobile scenarios as the algorithm described in I. The channel is modeled as Rayleigh channel. As we can see, the sum rate performance of the proposed NOMA scheme is close to that with perfect position knowledge, which is the upper bound of NOMA with partial channel information. And this is true under different user density and different transmission power. On the contrary, the performance of NOMA with users sorted randomly, which is the lower boundary of NOMA, is almost the same with OMA when the SNR is high. And the average sum rate of NOMA is superior to the OMA scheme in the medium to high SNR regions since the bandwidth resources in NOMA systems is shared by multiple users. However, in the very low SNR regions the interference signals may be not able to removed and several users cannot detect their messages correctly. This issue can be solved by more advanced power allocation strategy which is an interesting research topic in the future.

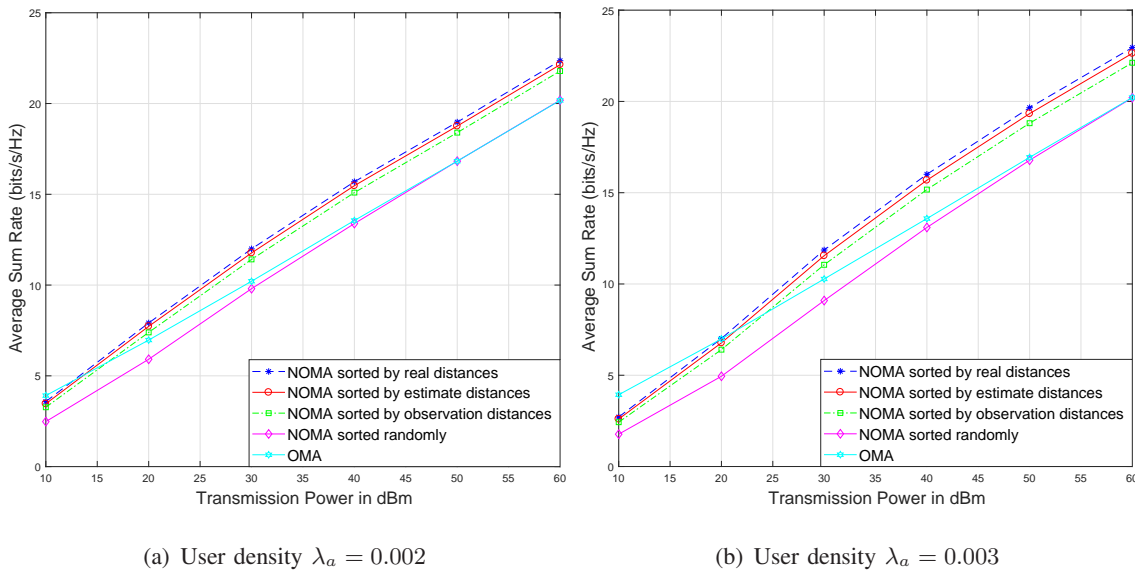


Fig. 6. Average sum rate performance of position-prediction based NOMA with observation noise variance $\sigma_{ob}^2 = 50$.

Fig. 6 illustrates the simulation results for sum rate performance of position-prediction based NOMA in mobile scenarios as the algorithm demonstrate in II. We use Rayleigh channel to model the channel condition. In our simulation setting, the slots in which the BS has access to observation data only account for about 25% in all transmission slots. As shown from Fig. 6(a) and Fig. 6(b), one can observe our proposed NOMA scheme with incomplete observation data still obtain an excellent sum rate performance. And in the meantime the communication overhead used to feedback channel information is largely reduced at the cost of negligible performance degradation. In other words, this scheme results in a trade off between system performance and complexity. And the performance of our scheme is still superior to the OMA as expected.

VI. CONCLUSION

In this paper, a position filtering-based NOMA scheme in mobile scenarios has been proposed. This scheme consists of two algorithms, i.e. position-tracking based NOMA and position-prediction based NOMA. The impact of estimated position deviation has been investigated and the simulation results validate the correctness of our analytical results. By comparing our scheme to the conventional NOMA and OMA schemes, the spectrum efficiency performance improvement can be observed from the Monte Carlo simulation results. Furthermore, an important future direction is to consider more advanced power allocation strategies combined with our proposed NOMA scheme.

APPENDIX A
PROOF FOR LEMMA 2

Recall that the distances of users U_1 and U_2 have $d_1 < d_2$, so we obtain $|r_1|^2 > |r_2|^2$ in the fading-free scenario. The two cases about the results of distance estimation are illustrated as follows

- (1) The distance estimation result is $\hat{d}_1 < \hat{d}_2$. In this situation, user U_2 regards the signal S_1 as interference and detect his own message directly. The user U_1 firstly considers his own signal S_1 as interference to detect S_2 and removes S_2 according to SIC strategy, then detects the signal S_1 . According to (8), the achievable rate of S_1 is limited to the channel condition of U_1 while the achievable rate of S_2 is constrained by the channel condition U_2 .
- (2) The distance estimation result is $\hat{d}_1 > \hat{d}_2$. In this context, the two receivers have a different detection process and the restriction of achievable rate also becomes different. In detail, the detection order is reverse. The user U_1 detects his signal S_1 with regarding S_2 as interference. The user U_2 detects the signal S_2 after removing the interference of S_1 . In this case, the achievable rates of both S_1 and S_2 are limited by U_2 because of its poor channel condition.

To make it clearer, we have shown the detection process and the signals that restrict the achievable rate (boldface) in table III.

TABLE III
RECEIVER DETECTION PROCESS IN THE FADING-FREE SCENARIO

	U_1	U_2
$\hat{d}_1 < \hat{d}_2$	$S_2 \rightarrow S_1$	S_2
$\hat{d}_1 > \hat{d}_2$	S_1	$S_1 \rightarrow S_2$

Based on table III, the sum rate performance of NOMA with partial channel information for the two pairing users is given as follows

$$R_{sum}^I = (1 - P_e)(R_1 + R_{1 \rightarrow 2}) + P_e(R_2 + R_{2 \rightarrow 1}) \quad (33)$$

Where the probability P_e has been formulated in Lemma 1. Substitute (4), (5) and (6) into (33),

we have

$$\begin{aligned}
R_{sum}^I &= \left[\log_2 (1 + \rho |r_1|^2 \alpha_1) + \log_2 \left(1 + \frac{|r_2|^2 \alpha_2}{|r_2|^2 \alpha_1 + \frac{1}{\rho}} \right) \right] \\
&\quad \times (1 - P_e) + P_e \times \left[\log_2 (1 + \rho |r_2|^2 \alpha_2) \right. \\
&\quad \left. + \log_2 \left(1 + \frac{|r_2|^2 \alpha_1}{|r_2|^2 \alpha_2 + \frac{1}{\rho}} \right) \right] \\
&= \left[\log_2 (1 + \rho |r_1|^2 \alpha_1) + \log_2 \left(1 + \frac{|r_2|^2 \alpha_2}{|r_2|^2 \alpha_1 + \frac{1}{\rho}} \right) \right] \\
&\quad \times (1 - P_e) + P_e \times \log_2 (1 + \rho |r_2|^2) \\
&= \log_2 \left(1 + \frac{|r_2|^2 \alpha_2}{|r_2|^2 \alpha_1 + \frac{1}{\rho}} \right) + P_e \log_2 (1 + \rho |r_2|^2 \alpha_1) \\
&\quad + (1 - P_e) \log_2 (1 + \rho |r_1|^2 \alpha_1)
\end{aligned} \tag{34}$$

Therefore, this completes the proof of lemma 2.

APPENDIX B

PROOF FOR LEMMA 3

In the fading scenario, the detection process and the restrictive factor of achievable rate become more complex due to the impact of small-scale fading. Using the similar method in the proof of Lemma 2, the detection process and the signals that restrict the achievable rate are listed in the table IV. Recall the optimal user order proposed in [15], it's better to detect the signals of

TABLE IV
RECEIVER DETECTION PROCESS IN THE FADING SCENARIO

	U_1	U_2
$ r_1 ^2 > r_2 ^2, \hat{d}_1 > \hat{d}_2$	S_1	$S_1 \rightarrow S_2$
$ r_1 ^2 < r_2 ^2, \hat{d}_1 < \hat{d}_2$	$S_2 \rightarrow S_1$	S_2
$ r_1 ^2 > r_2 ^2, \hat{d}_1 < \hat{d}_2$	$S_2 \rightarrow S_1$	S_2
$ r_1 ^2 < r_2 ^2, \hat{d}_1 > \hat{d}_2$	S_1	$S_1 \rightarrow S_2$

the weak users firstly. And from the table IV, one can observe that the detection order error

event occurs on the first two conditions. Let P_k ($k = 1, \dots, 4$) denotes the probability of each condition. As a result, the error probability in the fading scenario is given as follows

$$\begin{aligned}
P_e^2 &= P_1 + P_2 \\
&= \Pr \left(|r_1|^2 > |r_2|^2, \hat{d}_1 > \hat{d}_2 \right) \\
&\quad + \Pr \left(|r_1|^2 < |r_2|^2, \hat{d}_1 < \hat{d}_2 \right)
\end{aligned} \tag{35}$$

Due to the independence of channels and measurement, the probability is given by

$$\begin{aligned}
P_e^2 &= \Pr \left(|r_1|^2 > |r_2|^2 \right) \times P_e \\
&\quad + \left[1 - \Pr \left(|r_1|^2 > |r_2|^2 \right) \right] (1 - P_e)
\end{aligned} \tag{36}$$

Let $D = d_2^2/d_1^2$. With some algebraic manipulations, the probability term in (36) is calculated as

$$\Pr \left(|r_1|^2 > |r_2|^2 \right) = \Pr \left(|h_2|^2 < D |h_1|^2 \right) = \frac{D}{D+1} \tag{37}$$

By substituting (37) into (36), the first part of the lemma is proved.

In addition, the average sum rate can be expressed as

$$R_{sum}^I = \sum_{k=1}^4 \mathbb{E} \{ C_k \} P_k \tag{38}$$

Where

$$\begin{aligned} C_1 &= \log \left(1 + \frac{|r_2|^2 \alpha_1}{|r_2|^2 \alpha_2 + \frac{1}{\rho}} \right) + \log (1 + \rho |r_2|^2 \alpha_2) \\ &= \log (1 + \rho |r_2|^2) \end{aligned} \quad (39)$$

$$\begin{aligned} C_2 &= \log \left(1 + \frac{|r_1|^2 \alpha_2}{|r_1|^2 \alpha_1 + \frac{1}{\rho}} \right) + \log (1 + \rho |r_1|^2 \alpha_1) \\ &= \log (1 + \rho |r_1|^2) \end{aligned} \quad (40)$$

$$\begin{aligned} C_3 &= \log \left(1 + \frac{|r_2|^2 \alpha_2}{|r_2|^2 \alpha_1 + \frac{1}{\rho}} \right) + \log (1 + \rho |r_1|^2 \alpha_1) \\ &= \log (1 + \rho |r_2|^2) - \log (1 + \rho |r_2|^2 \alpha_1) \\ &\quad + \log (1 + \rho |r_1|^2 \alpha_1) \end{aligned} \quad (41)$$

$$\begin{aligned} C_4 &= \log \left(1 + \frac{|r_1|^2 \alpha_1}{|r_1|^2 \alpha_2 + \frac{1}{\rho}} \right) + \log (1 + \rho |r_2|^2 \alpha_2) \\ &= \log (1 + \rho |r_1|^2) - \log (1 + \rho |r_1|^2 \alpha_2) \\ &\quad + \log (1 + \rho |r_2|^2 \alpha_2) \end{aligned} \quad (42)$$

The key to obtain the average sum rate in (38) is to calculate the conditional expectation in each situation. Let random variable $X_k = |r_k|^2$ ($k = 1, 2$), and the first expectation term is calculated as follows.

$$\begin{aligned} & \mathbb{E} \left\{ C_1 | X_1 > X_2, \hat{d}_1 > \hat{d}_2 \right\} \\ &= \mathbb{E} \{ C_1 | X_1 > X_2 \} \\ &= \int_0^\infty \int_{x_2}^\infty C_1(x_2) f(x_1, x_2 | X_1 > X_2) dx_1 dx_2 \\ &= \frac{\int_0^\infty C_1(x_2) f_{X_2}(x_2) \left[\int_{x_2}^\infty f_{X_1}(x_1) dx_1 \right] dx_2}{\Pr(X_1 > X_2)} \\ &= \frac{\lambda_2 \rho}{\lambda \ln 2} \int_0^\infty \frac{e^{-\lambda x_2}}{1 + \rho x_2} dx_2 / \Pr(X_1 > X_2) \end{aligned} \quad (43)$$

Recall the following result

$$\int_0^\infty \frac{e^{-lx}}{1 + x\phi} dx = -\frac{l}{\phi} e^{\frac{l}{\phi}} \text{Ei} \left(-\frac{l}{\phi} \right) \quad (44)$$

Define $\varphi(n, \phi) = -\frac{\lambda_n}{\lambda \ln 2} e^{\frac{\lambda}{\phi}} \text{Ei}\left(-\frac{\lambda}{\phi}\right)$ and $\varphi'(n, \phi) = -\frac{1}{\ln 2} e^{\frac{\lambda}{\phi}} \text{Ei}\left(-\frac{\lambda_n}{\phi}\right)$. By substituting (37) and (44) into (43), we have

$$\text{E}\left\{C_1|X_1 > X_2, \hat{d}_1 > \hat{d}_2\right\} = \varphi(2, \rho) / \left(\frac{D}{D+1}\right) \quad (45)$$

Similar to (45), we can obtain other conditional expectations as follows

$$\text{E}\left\{C_2|X_1 < X_2, \hat{d}_1 < \hat{d}_2\right\} = \varphi(1, \rho) / \left(\frac{1}{D+1}\right) \quad (46)$$

$$\begin{aligned} \text{E}\left\{C_3|X_1 > X_2, \hat{d}_1 < \hat{d}_2\right\} &= [\varphi(2, \rho) - \varphi(2, \rho\alpha_1) \\ &+ \varphi'(1, \rho\alpha_1) - \varphi(1, \rho\alpha_1)] / \left(\frac{D}{D+1}\right) \end{aligned} \quad (47)$$

$$\begin{aligned} \text{E}\left\{C_4|X_1 < X_2, \hat{d}_1 > \hat{d}_2\right\} &= [\varphi(1, \rho) - \varphi(1, \rho\alpha_2) \\ &+ \varphi'(2, \rho\alpha_2) - \varphi(2, \rho\alpha_2)] / \left(\frac{1}{D+1}\right) \end{aligned} \quad (48)$$

With the same method like (36) and (37), the probability P_k ($k = 1, \dots, 4$) is obtained. And by substituting the result of P_k , (45), (46), (47) and (48) into (38), the lemma has been proved.

REFERENCES

- [1] L. Dai, B. Wang, Z. Ding, Z. Wang, S. Chen, and L. Hanzo, "A survey of non-orthogonal multiple access for 5g," *IEEE Communications Surveys & Tutorials*, 2018.
- [2] Y. Saito, A. Benjebbour, Y. Kishiyama, and T. Nakamura, "System-level performance evaluation of downlink non-orthogonal multiple access (noma)," in *Personal Indoor and Mobile Radio Communications (PIMRC), 2013 IEEE 24th International Symposium on*. IEEE, Conference Proceedings, pp. 611–615.
- [3] "Study on downlink multiuser superposition transmission for lte," *document, 3rd Generation Partnership Project (3GPP)*, March 2016.
- [4] L. Zhang, W. Li, Y. Wu, X. Wang, S.-I. Park, H. M. Kim, J.-Y. Lee, P. Angueira, and J. Montalban, "Layered-division-multiplexing: Theory and practice," *IEEE Transactions on Broadcasting*, vol. 62, no. 1, pp. 216–232, 2016.
- [5] L. Zhang, Y. Wu, W. Li, K. Salehian, S. Lafleche, X. Wang, S. I. Park, H. M. Kim, J.-y. Lee, and N. Hur, "Layered-division multiplexing: An enabling technology for multicast/broadcast service delivery in 5g," *IEEE Communications Magazine*, vol. 56, no. 3, pp. 82–90, 2018.
- [6] Z. Ding, Z. Yang, P. Fan, and H. V. Poor, "On the performance of non-orthogonal multiple access in 5g systems with randomly deployed users," *IEEE Signal Processing Letters*, vol. 21, no. 12, pp. 1501–1505, 2014.
- [7] Z. Ding, P. Fan, and H. V. Poor, "Impact of user pairing on 5g nonorthogonal multiple-access downlink transmissions," *IEEE Trans. Vehicular Technology*, vol. 65, no. 8, pp. 6010–6023, 2016.
- [8] S. Timotheou and I. Krikidis, "Fairness for non-orthogonal multiple access in 5g systems," *IEEE Signal Processing Letters*, vol. 22, no. 10, pp. 1647–1651, 2015.
- [9] M. Al-Imari, P. Xiao, M. A. Imran, and R. Tafazolli, "Uplink non-orthogonal multiple access for 5g wireless networks," in *Wireless Communications Systems (ISWCS), 2014 11th International Symposium on*. IEEE, Conference Proceedings, pp. 781–785.

- [10] J. Choi, "Non-orthogonal multiple access in downlink coordinated two-point systems," *IEEE Communications Letters*, vol. 18, no. 2, pp. 313–316, 2014.
- [11] Z. Ding, F. Adachi, and H. V. Poor, "The application of mimo to non-orthogonal multiple access," *IEEE Transactions on Wireless Communications*, vol. 15, no. 1, pp. 537–552, 2016.
- [12] Z. Ding, M. Peng, and H. V. Poor, "Cooperative non-orthogonal multiple access in 5g systems," *IEEE Communications Letters*, vol. 19, no. 8, pp. 1462–1465, 2015.
- [13] Y. Liu, Z. Ding, M. ElKashlan, and J. Yuan, "Nonorthogonal multiple access in large-scale underlay cognitive radio networks," *IEEE Transactions on Vehicular Technology*, vol. 65, no. 12, pp. 10 152–10 157, 2016.
- [14] H. Marshoud, V. M. Kapinas, G. K. Karagiannidis, and S. Muhaidat, "Non-orthogonal multiple access for visible light communications," *IEEE Photon. Technol. Lett*, vol. 28, no. 1, pp. 51–54, 2016.
- [15] Z. Yang, W. Xu, C. Pan, Y. Pan, and M. Chen, "On the optimality of power allocation for noma downlinks with individual qos constraints," *IEEE Communications Letters*, vol. 21, no. 7, pp. 1649–1652, 2017.
- [16] Z. Yang, Z. Ding, P. Fan, and G. K. Karagiannidis, "On the performance of non-orthogonal multiple access systems with partial channel information," *IEEE Transactions on Communications*, vol. 64, no. 2, pp. 654–667, 2016.
- [17] Y. Liu, Z. Ding, M. ElKashlan, and H. V. Poor, "Cooperative non-orthogonal multiple access with simultaneous wireless information and power transfer," *IEEE Journal on Selected Areas in Communications*, vol. 34, no. 4, pp. 938–953, 2016.
- [18] Z. Ding, P. Fan, and H. V. Poor, "Random beamforming in millimeter-wave noma networks," *IEEE access*, vol. 5, pp. 7667–7681, 2017.
- [19] R. E. Kalman, "A new approach to linear filtering and prediction problems," *Journal of basic Engineering*, vol. 82, no. 1, pp. 35–45, 1960.
- [20] F. Gustafsson and F. Gunnarsson, "Mobile positioning using wireless networks: possibilities and fundamental limitations based on available wireless network measurements," *IEEE Signal processing magazine*, vol. 22, no. 4, pp. 41–53, 2005.
- [21] Z. Ding, P. Fan, G. K. Karagiannidis, R. Schober, and H. V. Poor, "Noma assisted wireless caching: Strategies and performance analysis," *IEEE Transactions on Communications*, 2018.
- [22] I. S. Gradshteyn and I. M. Ryzhik, *Table of integrals, series, and products*. Academic press, 2014.
- [23] Z. R. Zaidi and B. L. Mark, "Real-time mobility tracking algorithms for cellular networks based on kalman filtering," *IEEE Transactions on Mobile Computing*, vol. 4, no. 2, pp. 195–208, 2005.